# CRITERIA FOR DYNAMIC CRACK CURVING AND BRANCHING

**M. Ramulu and A. S. Kobayashi**

*University of Washington, Department of Mechanical Engineering, Seattle, WA 98195, USA*

## ABSTRACT

The dynamic crack curving and crack branching criteria with modifications are presented. The modified crack curving and branching criteria are verified with the dynamic photoelastic experiments involving Homalite-100 and polycarbonate fracture specimens. Crack curving was consistently observed when the characteristic distance $r_o \leq r_c$ and branching was observed when the necessary condition of $K_I \geq K_{Ib}$ and sufficient condition of $r_o \leq r_c$ were satisfied simultaneously. The crack branching criterion is then used to predict crack branching in a pressurized metal pipe.

## KEY WORDS

Dynamic fracture, crack curving, crack branching, branching angle, crack tip stress field, branching stress intensity factor, characteristic distance, dynamic finite element method, dynamic photoelasticity.

## INTRODUCTION

The analytical models which describe crack propagation, either from an energistic standpoint or through the crack tip stress state, assume that a straight crack will continue to propagate straight under symmetric loading and boundary conditions. Experimental evidence, however, shows that even under these conditions, the crack tended to deviate from its straight path either by gradually curving or by sudden splitting into two or more branch cracks. Experimental evidence on crack curving and crack branching can be found in Rossmanith (1980), Ravichandra (1982) and Ramulu and Kobayashi (1983). Recently, the authors proposed a dynamic crack curving (Ramulu and Kobayashi, 1983) and branching (Ramulu, Kobayashi and Kang, 1982) criteria based on the directional stability of a propagating crack. This criteria incorporates, in principle, crack-tip microcracking which governs the direction of crack growth. Such micro-cracking is shown schematically in Fig. 1 where micro-crack nucleation, growth, and interaction, which effectively blunts the crack tip, are triggered by the singular stress field. Load shedding due to blunting then activates off-axis micro-cracks which tend to divert the crack away

from its original direction of self-similar crack extension. The crack-tip stress parameters, which control the locations and orientations of these off-axis micro-cracks, are the mixed-mode stress intensity factors and the remote stress component which is the first non-singular term in the crack tip stress field. Larger stress intensity factors generates more bluntness with higher stored energy which, upon release, causes multiple-crack extension. As shown in Fig. 1, a single crack tip diversion under lower stress intensity factor results in crack curving and a multiple crack tip diversion under higher stress intensity factor results in crack branching.

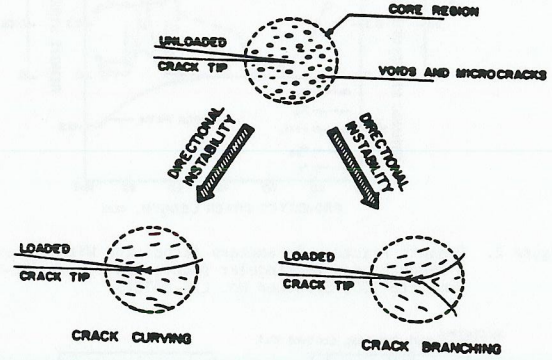


Figure 1. Crack Curving and Branching Mechanisms

In the following, brief reviews of the theoretical background of crack curving and crack branching criteria are given. These criteria are then verified by dynamic photoelastic results of crack curving and branching in Homalite-100 and polycarbonate fracture specimens. Finally, the crack branching criterion is used to predict crack branching results in a pressurized metal pipes.

## DYNAMIC CRACK CURVING CRITERION

The authors have used both the maximum circumferential stress criterion (1983a) and the minimum strain energy density criterion (1983b) in predicting crack curving. The crack curving angles predicted by using either of the two fracture criteria are nearly identical for lower values of mode II stress intensity factor, $K_{II}$, and thus only the circumferential stress criterion will be used in this paper. The near field, circumferential stress, $\sigma_{\theta\theta}$ of a mixed-mode crack-tip propagating at constant velocity is given in terms of a local crack-tip coordinate as (Freund, 1976):

$$\sigma_{\theta\theta} = \frac{K_I}{\sqrt{2\pi}} B_I \left[ \left[ (S_1^2-S_2^2)-(1+S_1^2)\cos 2\theta \right) \frac{\cos\frac{\theta_1}{2}}{\sqrt{r_1}} + \frac{4S_1S_2}{1+S_2^2}\cos 2\theta \frac{\cos\frac{\theta_2}{2}}{\sqrt{r_2}} - 2S_1 \sin 2\theta \left( \frac{\sin\frac{\theta_1}{2}}{\sqrt{r_1}} - \frac{\sin\frac{\theta_2}{2}}{\sqrt{r_2}} \right) \right]$$

$$+ \frac{K_{II}}{\sqrt{2\pi}} B_{II} \left[ -2S_1 \sin 2\theta \frac{\cos\frac{\theta_1}{2}}{\sqrt{r_1}} + \frac{(1+S_2^2)^2}{2S_2} \sin 2\theta \frac{\cos\frac{\theta_2}{2}}{\sqrt{r_2}} + \left( (S_2^2-S_1^2) + (1+S_1^2)\cos 2\theta \right) \frac{\sin\frac{\theta_1}{2}}{\sqrt{r_1}} - (1+S_2^2)\cos 2\theta \frac{\sin\frac{\theta_2}{2}}{\sqrt{r_2}} \right] + \frac{\sigma_{ox}}{2}(1-\cos 2\theta) \quad (1)$$

where

$$S_1^2 = 1 - \frac{c^2}{c_1^2} \; ; \; S_2^2 = 1 - \frac{c^2}{c_2^2} \; ; \; r_1^2 = x^2 + S_1^2 y^2 ; \; r_2^2 = x^2 + S_2^2 y^2 ; \; \tan\theta_1 = \frac{S_1 y}{x} \; ; \; \tan\theta_2 = \frac{S_2 y}{x}$$

$$B_I = \frac{(1+S_2^2)}{4S_1S_2-(1+S_2^2)^2} \; ; \; B_{II} = \frac{2S_2}{4S_1S_2-(1+S_2^2)^2}$$



$K_I$ and $K_{II}$ are the modes I and II dynamic stress intensity factors and c, $c_1$ and $c_2$ are the crack velocity, dilatational and distortional stress wave velocities, respectively. $\sigma_{ox}$ is the remote stress or the non-singular stress acting in the direction of crack propagation. Crack curving occurs when the circumferential stress, $\sigma_{\theta\theta}$, at an inclined distance of r away from the propagating crack reaches an extremum value. The extremum condition for $\sigma_{\theta\theta}$, which is derived from Equation (1), with $K_{II} = 0$, yields a functional relation between the r and $\theta$ as (Ramulu, Kobayashi and Kang, 1982):

$$r = f(K_I, \sigma_{ox}, \theta, c, c_1, c_2) \quad (2)$$

The above relation can be used to determine the crack curving angle under given $K_I$, r and positive $\sigma_{ox}$ (Ramulu and co-workers, 1983). By setting $\theta = 0$ in this relation the following condition for self-similar crack extension is obtained:

$$r_o = \frac{1}{128\pi} \left[ \left( \frac{K_I}{\sigma_{ox}} \right) V_o(c, c_1, c_2) \right]^2 \quad (3)$$

where

$$V_o(c,c_1,c_2) = [B_1(c)\{-(1+S_2^2)(2-3S_1^2) - \frac{4S_1S_2}{1+S_2^2}(14+3S_2^2)+16(1+S_1S_2)\}]$$

Ramulu and Kobayashi's (1983) crack stability criterion, which is a dynamic extension of Streit and Finnie's (1980) static crack directional stability criterion, assumes that the crack will propagate straight when the above characteristic distance of $r_o$ is larger than a material parameter of $r_c$. When $r_o$ is less than $r_c$ and $\sigma_{ox} > 0$, the crack suddenly becomes unstable and will veer off in the non-zero $\theta_c$ direction which is determined from Equation (2). Detailed studies on the variations in this crack kinking angle with respect to variations in fracture parameters are found in Ramulu and Kobayashi (1983a and b).

Thus, the crack curving criterion can be summarized as:

$$K_{IC} \leq K_I < K_{Ib}$$

$$r_o \leq r_c$$

where $K_{IC}$ is the dynamic fracture toughness of the material and $K_{Ib}$ is the

critical branching stress intensity factor. The crack curving angle can be determined from the experimentally determined fracture parameters of $r_c$ and $K_I$ from the relation given in Equation (2) for positive $\sigma_{ox}$.

## DYNAMIC CRACK BRANCHING CRITERION

The dynamic crack branching criterion requires as a necessary condition, sufficient released strain energy for generating simultaneously, multiple cracks. Thus a critical stress intensity factor, $K_{Ib}$, is implicated in this necessary condition.

In order to generate multiple crack simultaneously, these cracks must branch from thier original self-similar crack propagation path. Thus, crack curving is introduced as a sufficiency condition.

The crack branching criterion can be summarized as:

$$K_I \geq K_{Ib} \qquad \text{Necessary condition}$$

$$r_o \leq r_c \qquad \text{Sufficient condition}$$

The crack kinking angle determined from the sufficiency condition is one half of the crack branching angle, and can be determined from the latter crack curving criterion for a positive $\sigma_{ox}$.

## DYNAMIC CRACK CURVING IN PHOTOELASTIC SPECIMENS

The validity of the above crack curving criterion was verified by dynamic photoelasticity results of Homalite-100 (Ramulu and Kobayashi, 1983) and polycarbonate (Sun and Co-workers, 1982) fracture specimens. In the following, one typical result from each of the above series of experiments will be shown.

Figure 2 shows the curved crack and the associated dynamic $K_I$, $K_{II}$, $\sigma_{ox}$, and $r_o$ in a Homalite-100, wedge-loaded, rectangular double-cantilever beam (WLRDCB) specimen of 9.5-mm thick and 76.2 x 152.4 mm with a blunt initial crack of length 2.4 mm (Ramulu and Kobayashi, 1983). The experimental details of this series of tests can be found in Kobayashi, Mall and Lee, (1976). While continuous fluctuations in the dynamic parameters are noted along the crack path, $r_o$ attained its minimum values at the onset of curving at midway and during the severe crack curving in the terminal stage of crack propagation. The results of nine crack curving experiments of Homalite-100 yielded an average value for the material parameter, $r_c$ of 1.3 mm.

Figure 3 shows specimen configurations and crack paths of five polycarbonate double edge crack tension specimens with either offset parallel cracks, offset slanted cracks or symmetrically located twin cracks which were used in this dynamic photoelastic study. The annealed thin polycarbonate specimens with blunt starter cracks exhibited brittle fracture with shear lips less than 10 percent of the thickness and an apparent crack tip yield zone of less than 1.5 mm. Also shown in Fig. 3 are the curved crack path fractures. The average $r_c$ value was 0.5 mm and is consistent with the $r_c$ estimated by Theocaris (1980).

The range of fracture parameters associated with this series of crack curving experiments on Homalte-100 and polycarbonate are summarized in Table 1. The



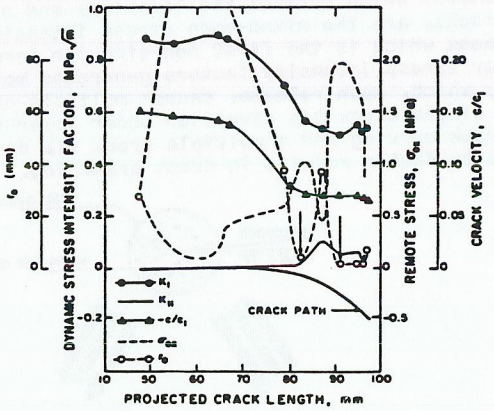


Figure 2. Dynamic Fracture Parameters Associated With a Curved Crack in a Wedge Loaded Rectangular Double Cantilever (WL-RDCB) Specimen, Homalite-100, Specimen No. L7B-051573

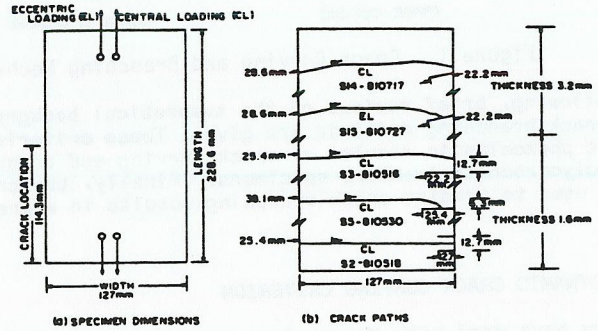


Figure 3. Polycarbonate Double Edged Crack Tension Specimen

TABLE 1 SUMMARY OF EXPERIMENTAL AND THEORETICAL RESULTS OF CRACK CURVING

| | HOMALITE-100 | POLYCARBONATE |
|---|---|---|
| Total Number of Experiments: | 9 | 5 |
| Type of Fracture Specimens: | DTT, SEN, WLRDCB | Double Edge Crack Spec. |
| Number of Data Points: | 81 | 114 |
| Crack Velocity, $c/c_1$: | About 0.21 | About 0.22 |
| $K_I$ (MPa$\sqrt{m}$): | 0.50 to 1.59 | 1.5 to 3.2 |
| $K_{II}/K_I$ | -0.22 to 0.18 | -0.33 to 0.19 |
| $\sigma^{ox}/K_I$: | 2.89 to 4.04 | -11.1 to 2.5 |
| $r_o^{ox}$(mm): | 1.0 to 1.5 | 0.25 to 0.75 |
| Measured Crack Curving Angle: | -20 to 26 degrees | -20 to 3 degrees |
| Predicted Crack Curving Angle: | -20 to 25 degrees | -19 to 5 degrees |

theoretically predicted crack curving angles, either in pure mode I or mode I and mode II loading conditions, in the presence of $\sigma_{ox}$, were within one degree of the corresponding measured values.

## DYNAMIC CRACK BRANCHING IN PHOTOELASTIC SPECIMENS

Figure 4 shows the variations in dynamic $K_I$, $K_{II}$ and $r_o$ in a fracturing singled edge notch (SEN), Homalite-100 specimen of 9.5 mm thick and 254 x 254 mm in size (Ramulu, Kobayashi and Kang, 1982). The experimental details of this series of tests are given in Kobayashi and co-workers, (1974). The crack, which started from a blunt initial crack, arrested after branching. By extrapolating the $K_I$ before and after branching, a $K_{Ib}$ = 2.0 MPa$\sqrt{m}$ and after branching $K_I$ = 0.9 MPa$\sqrt{m}$ are obtained. The $r_o$ reached an estimated minimum value of 1.3 mm at branching. The results of the other five experiments (Ramulu, Kobayashi and Kang, 1982) yielded an average $r_o$ of 1.3 mm at branching and a $K_{Ib}$ = 2.04 MPa$\sqrt{m}$. At the onset of crack branching, the crack velocity was found to be about 0.18 $c_1$. This $K_{Ib}$, which is approximately 4.9 times the fracture toughness of Homalite-100, is in agreement with the measured $K_{Ib}$ of Dally (1979).

Figure 5 shows the $K_I$, $K_{II}$ and $\sigma_{ox}$ variations in a 3.2 mm thick, 127 x 127 mm polycarbonate, single edge notch specimen with a blunt starter crack (Ramulu and co-workers, 1983). $K_{Ib}$ = 3.3 MPa$\sqrt{m}$ and an after $K_I$ = 2.2 MPa$\sqrt{m}$ were obtained by extrapolating the $K_I$ curve. While $K_{II}$ remained small prior to branching, a $K_{II}$ = 0.9 MPa$\sqrt{m}$ was obtained immediately after branching. The crack velocity at the onset of branching in this material was found to be about 0.24 $c_1$. This series of five crack branching experiments yielded an average value of $K_{Ib}$ = 3.3 MPa$\sqrt{m}$ and $r_c$ = 0.7 mm for this material.

In the SEN specimens, the energistic requirement for multiple cracking was satisfied but the crack curving criterion could not be satisfied since $\sigma_{ox}$ < 0, $K_{II}$ = 0. Under such conditon, $\sqrt{r_c}\,\sigma_{\theta\theta}/K_I$ is maximum at $\theta$ = 0 for the crack velocity of $c/c_1$ < 0.32. However, the reduction in angular stress distribution of $\sqrt{r_c}\,\sigma_{\theta\theta}/K_I$ at $\theta = \pm$ (10-14) degrees is a mere 1.7 - 3.5% which allows the crack to still bifurcate and double its energy release rate. Therefore, the predicted crack branching angle with crack curving is, at best, an estimated angle (Ramulu and co-workers, 1983). The summary of crack branching results on Homalite-100 and polycarbonate material is given in Table 2. It is interesting to observe that the branching stress intensity factor appears to be independent of the thickness as well as the initial and branching crack lengths. Also note that the deviation between the estimated and measured crack branching angles was 6 degrees and the average deviation was 3 degrees.

The crack curving as well as the crack branching criteria are also applicable to quasi-static problems. The crack branching criterion was thus used to evaluate branching data of 76 x 152 x 9.5 mm thick Homalite-100, wedge loaded, rectangular double cantilever beam specimens (Ramulu, Kobayashi and Kang, 1982). Since the cracks immediately branched from the blunt starter crack upon crack initiation, the necessary and sufficient conditions for branching were deduced by static-finite element analysis. Extreme bluntness of the starter crack render $K_{Ib}$ values meaningless and thus only the crack branching angles were considered. Table 3 summarizes the results of six tests where excellent agreement between the predicted and measured branch angles are noted.



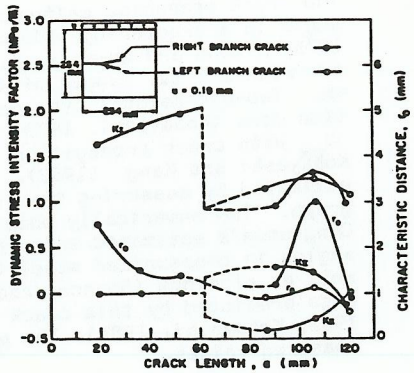


Figure 4. Modes I and II Dynamic Stress Intensity Factor and $r_o$ of Branched Cracks in Single Edged Crack Tension Specimen. (# B7)

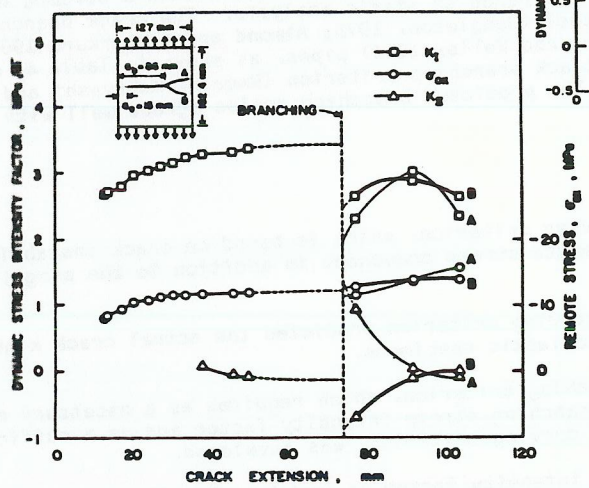


Figure 5. Modes I and II Dynamic Stress Intensity Factors & $\sigma_{ox}$ of Branched Cracks in Single Edged Crack Tension Specimen. (#KB-820826-1)

TABLE 2 SUMMARY OF CRACK BRANCHING DATA IN HOMALITE-100 AND POLYCARBONATE SINGLE EDGED NOTCH TENSION SPECIMENS

| Test No. | Specimen Thickness h mm | Initial Crack Length $a_o$ mm | Crack Length at Branching $a_b$ mm | $K_{Ib}$ MPa$\sqrt{m}$ | $\sigma_{ox}$ MPa | $r_c$ mm | Branching Angle $2\theta_c$ Measd. Degrees | Branching Angle $2\theta_c$ Est. Degrees |
|---|---|---|---|---|---|---|---|---|
| HOMALITE-100 | | | | | | | | |
| B8 | 3.18 | 5.6 | 66.0 | 2.08 | -6.93 | 1.2 | 23 | 26 |
| B9 | 3.18 | 4.3 | 177.0 | 2.03 | -5.55 | 1.3 | 30 | 24 |
| W082270 | 3.58 | 5.8 | 139.7 | 2.03 | -6.75 | 1.4 | 26 | 26 |
| B7 | 9.53 | 5.1 | 52.6 | 2.00 | -6.80 | 1.4 | 30 | 28 |
| B5 | 9.53 | 13.5 | 19.1 | 2.08 | -7.08 | 1.2 | 30 | 28 |
| B6 | 9.53 | 13.5 | 28.7 | 2.09 | -7.60 | 1.3 | 28 | 32 |
| | | | Average | 2.04 | -6.70 | 1.3 | 27.8 | 27.3 |
| POLYCARBONATE | | | | | | | | |
| KB-820826-1 | 3.2 | 15 | 86 | 3.3 | -11.50 | 0.85 | 34 | 31 |
| KB-820816-2 | 6.4 | 9 | 52 | 3.2 | -11.48 | 0.78 | 22 | 28 |
| KB-820822 | 3.2 | 16 | 65 | 3.3 | -11.18 | 0.78 | 29 | 26 |
| KB-820824 | 3.2 | 15 | 41 | 3.4 | -14.72 | 0.58 | 25 | 26 |
| | | | Average | 3.3 | -12.22 | 0.75 | 27.5 | 27.8 |

## CRACK BRANCHING IN PRESSURIZED PIPES

The crack branching criterion was also used to predict the crack branching angle in a fracturing thin mild steel tube which burst at -120° C (Congleton, 1973; Almond and co-workers, 1969). The pipe was 12.7 mm thick, 152 mm diameter with a total length of 457.2 mm and a central through crack of 2a = 57.2 mm. Two-dimensional dynamic finite element analysis was used in its generation mode (Kobayashi, 1979) to determine numerically the dynamic $K_{ID}$ and the $\sigma_{ox}$ with crack propagation. Details of this analysis are found in Ramulu, Kobayashi and Kang (1982). The characteristic $r_c$ = 1 mm for this steel was estimated by measuring the lengths of the secondary cracks in the photomicrograph. The numerically obtained $K_{Ib}$ = 124 MPa$\sqrt{m}$ was within 5 percent of Congleton's estimated value based on static analysis. The crack branching angles in pressurized steel (Congleton, 1973; Almond and co-workers 1969) as well as aluminum (Shannon and Wells, 1974) pipes, as shown in Table 4, were also predicted by this crack branching criterion (Ramulu, Kobayashi and Kang, 1982; Kobayashi, 1983). The predicted branching angles agreed well with the measured values.

## CONCLUSIONS

1. A dynamic crack curving criterion, which is based on crack instability and which involves the remote stress component in addition to the singular stresses, was developed.

2. This dynamic crack curving criterion predicted the actual crack kinking angles in fracturing photoelastic specimens.

3. A dynamic crack branching criterion, which requires as a necessary condition a critical crack branching stress intensity factor and as a sufficient condition the above crack curving criterion, was developed.

4. The branching stress intensity factor is found to be independent of thickness as well as initial and branching crack lengths of the fractured specimens.

5. This dynamic crack branching criterion predicted the actual crack branching angle in dynamically as well as statically fracturing photoelastic specimens. It also predicted the crack branching angle in a bursting metal pipe.

## REFERENCES


Rossmanith, H. P. (1980). "Crack Branching of Brittle Materials, Part I", University of Maryland Report, 1977-1980.

Ravi Chandra, K. (1982). "An Experimental Investigation into the Mechanics of Dynamic Fracture", Ph.D. Thesis, California Institute of Technology.

Ramulu, M. and Kobayashi, A. S. (1983a). "Dynamic Crack Curving - A Photoelastic Evaluation", Experimental Mechanics, Vol. 23, pp. 1-9.

Ramulu, M., Kobayashi, A. S. and Kang, B. S.-J. (1982). "Dynamic Crack Branching - A Photoelastic Evaluation", presented at the Fifteenth National Symposium on Fracture Mechanics, University of Maryland.

Ramulu, M. and Kobayashi, A. S. (1983b). "Strain Energy Density Fracture Criterion in Elastodynamic Mixed Mode Crack Propagation", Engineering Fracture Mechanics, 18, pp. 1087-1098.

Freund, L. B. (1976). "Dynamic Crack Propagation", Mechanics of Fracture, ed. by F. Erdogan, ASME, Vol. 19, pp. 105 - 134.





Ramulu, M., Kobayashi, A. S., Kang, B. S.-J. and Barker, D. B. (1983). "Further Studies on Dynamic Crack Branching", Experimental Mechanics, Vol. 23, pp. 431-437.

Streit, R. and Finnie, I. (1980). "An Experimental Investigation of Crack Path Directional Stability", Experimental Mechanics, Vol. 20, pp. 17 - 23.

Sun, Y.-J., Ramulu, M., Kobayashi, A. S., and Kang, B. S.-J. (1982) "Further Studies on Dynamic Crack Curving", Developments in Theoretical and Applied Mechanics, edt. by T. J. Chung and G. R. Karr, The University of Alabama Press, Huntsville, Vol. 11, pp. 203 - 218.

Kobayashi, A. S., Mall, M. and Lee, M. H. (1976). "Fracture Dynamics of Wedge-Loaded Double Cantilever Beam Specimen", Cracks and Fracture, ASTM STP 601, pp. 274 - 290.

Theocaris, P. S. (1980). "The Caustic as a Means to Define the Core Region in Brittle Fracture", Engineering Fracture Mechanics, Vol. 12, pp. 235 - 242.

Kobayashi, A. S., Wade, B. G., Bradley, W. B. and Chiu, S. T. (1974). "Crack Branching in Fracturing Homalite - 100 Plates", Engineering Fracture Mechanics, Vol. 6, pp. 81 - 92.

Dally, J. W. (1979). "Dynamic Photoelastic Studies of Fracture", Experimental Mechanics, Vol. 19, pp. 349 - 367.

Congleton, J. (1973). "Practical Applications of Crack-Branching Measurements", Dynamic Crack Propagation, ed. by G. C. Sih, Noordhoff International Publishing, Leyden, pp. 427 - 438.

Almond, E. A., Petch, N. J., Wraith, A. E. and Wright, E. S. (1969). "The Fracture of Pressurized Laminated Cylinders", Journal of Iron and Steel Institute, Vol. 207, pp. 1319 - 1323.

Kobayashi, A. S. (1979). "Dynamic Fracture Analysis by Dynamic Finite Element Method - Generation and Propagation Analysis", Nonlinear and Dynamic Fracture Mechanics, ed. by N. Perrone and S. N. Atluri, ASME AMD Vol. 35, pp. 19 - 36.

Ramulu, M., Kobayashi, A. S., and Kang, B. S.-J. (1982b). "Dynamic Crack Curving and Branching in Line-Pipe", ASME Journal of Pressure Vessel Technology, Vol. 104, pp. 317 - 322.

Shannon, R. W. E. and Wells, A. S. (1974). "A Study of Ductile Crack Propagation in Gas Pressurized Pipeline", Proc. of Int. Symp. on Pipe Line, paper No. 17, New Castle Upon Tyne.

Kobayashi, A. S. (1983). "Crack Branching, Crack Arrest and Rapid Tearing", Proc. of NSF Workshop on Dynamic Fracture, ed. by W. G. Knauss, Cal. Tech..


TABLE 3 SUMMARY OF CRACK BRANCHING ANGLE DISTRIBUTION IN A WEDGE LOADED RECTANGULAR DOUBLE CANTILEVER BEAM SPECIMEN

| Test No. | Specimen Thickness h mm | Diameter of Blunt Notch ρ mm | Measured Branch Angle $2\theta_c$ | Calculated 1st Branch Angle 1st Branching $2\theta_c$ |
|---|---|---|---|---|
| L6B-120573 | 9.5 | 2.2 | 52 | 52 |
| L10B-052473 | 9.5 | 2.2 | 52 | 52 |
| L14B | 9.5 | 5.0 | 55 | 52 |
| L19B-013074 | 9.5 | 4.0 | 54 | 52 |
| L27B-022474 | 9.5 | 2.4 | 54 | 52 |
| | | Average | 53.4 | 52 |

TABLE 4 CRACK BRANCHING DATA IN PRESSURIZED METAL PIPES

| Material | Branching $K_{Ib}$ MPa$\sqrt{m}$ | Branching $r_c$ mm | Branching Angle Measured $2\theta_c$ | Branching Angle Predicted $2\theta_c$ |
|---|---|---|---|---|
| Steel | 124 | 1 | 66 | 64 |
| Aluminum | xxx | 1.3 | 88 | 84 |